

Path-Extrema Upper Bounds on Mean Entropy Production

Surachate Limkumnerd¹

¹*Department of Physics, Faculty of Science, Chulalongkorn University, Bangkok 10330, Thailand*
(Dated: May 19, 2026)

Fluctuation relations imply the second-law inequality $\langle \Sigma_T \rangle \geq 0$, but path extrema can also constrain how large the mean entropy production can be. For steady-state processes with entropy-production martingale $M_t = e^{-\Sigma_t}$, we show that knowing only the positive running maximum of Σ_t gives no improvement over the trivial endpoint bound: rare negative entropy-production excursions can still carry the exponential weight required by the fluctuation relation. Using the running extrema $L_T = \inf M_t$ and $H_T = \sup M_t$, we derive a path-extrema upper envelope \mathcal{U}_{ext} . The relaxed envelope problem ranks realized intervals by the entropy gain per martingale cost, $\ln(H_T/L_T)/(H_T - L_T)$, giving a continuous knapsack problem. The actual mean satisfies the exact identity $\langle \Sigma_T \rangle = \mathcal{U}_{\text{ext}} - \mathcal{A} - \mathcal{C}$, where \mathcal{A} is an allocation gap across realized envelopes and \mathcal{C} is a curvature gap within each envelope. Thus path extrema set the upper envelope, while the two gaps quantify how actual dynamics allocate terminal outcomes across envelope classes and place terminal values within each realized envelope. This turns path-extrema information into a quantitative upper-bound theory for entropy production, complementary to the usual lower-bound role of fluctuation relations.

I. INTRODUCTION

The second law of thermodynamics is often expressed, in stochastic thermodynamics, as the nonnegativity of the mean total entropy production,

$$\langle \Sigma_T \rangle \geq 0.$$

At the trajectory level, however, entropy production is a fluctuating quantity. Individual trajectories may have negative entropy production even though the ensemble mean is nonnegative. This coexistence of typical irreversibility and rare entropy-consuming fluctuations is encoded in fluctuation relations. In particular, the integral fluctuation theorem gives

$$\langle e^{-\Sigma_T} \rangle = 1,$$

from which the second-law inequality follows immediately by Jensen's inequality [1].

Most refinements of the second law have focused on lower bounds associated with this inequality. Thermodynamic uncertainty relations bound the entropy production required to achieve a given current precision [2–4]. Thermodynamic speed limits bound the dissipation required to transform probability distributions in finite time [5, 6]. Thermodynamic inference methods use partial trajectory data, visible transitions, waiting times, or moments to infer lower bounds on entropy production when the full microscopic dynamics is inaccessible [7–10]. These developments have made entropy production not merely a sign-constrained quantity, but a quantitative cost constrained by fluctuations, precision, and observability.

The complementary upper-bound question has received less attention. Given information about the stochastic entropy production itself, how large can $\langle \Sigma_T \rangle$ be? This question is not answered by the integral fluctuation theorem alone. The identity $\langle e^{-\Sigma_T} \rangle = 1$ strongly

constrains the negative tail of Σ_T , but it does not by itself say how large the mean may be once only partial information about the trajectory is retained. In earlier work, an upper bound on the mean entropy production was obtained from the extrema of stochastic entropy production together with the fluctuation theorem [11]. That result used the convexity of $-\ln x$ to complement the Jensen lower bound. Other upper bounds have recently been obtained from kinetic information such as dynamical activity and transition-rate ratios [12]. Here we instead use path extrema of the exponential entropy-production process $e^{-\Sigma_t}$. Subsequent developments in martingale stochastic thermodynamics have clarified the importance of entropy-production infima, stopping times, and running extrema [13–19]. These developments suggest that upper bounds should not be viewed only as endpoint support bounds. They should also be understood as constraints imposed by the extrema reached along the path.

This paper develops that viewpoint. We consider steady-state stochastic thermodynamic processes for which

$$M_t = e^{-\Sigma_t}$$

is a positive martingale with $M_0 = 1$. Physically, this means that the exponential entropy production is not merely normalized at one final time; its conditional future average is fixed by its present value. This setting includes standard stationary Markov jump processes with local detailed balance, and also diffusion processes under the usual regularity conditions for stochastic thermodynamics [20], when Σ_t denotes the total entropy production relative to the steady-state dynamics. In a Markov jump process, for example, Σ_t is the log ratio between the probability of a realized trajectory and that of its time-reversed counterpart. The process $e^{-\Sigma_t}$ is then a Radon–Nikodym density process, and hence a positive martingale with respect to the natural trajectory filtration.

This martingale property is stronger than the fixed-time integral fluctuation theorem and is the basis of several universal results on entropy-production extrema and stopping times [14, 18, 19]. We define the running martingale envelope by

$$L_T = \inf_{0 \leq t \leq T} M_t, \quad H_T = \sup_{0 \leq t \leq T} M_t.$$

Equivalently, in entropy-production variables,

$$A_T = -\ln L_T = \sup_{0 \leq t \leq T} \Sigma_t, \quad B_T = \ln H_T = -\inf_{0 \leq t \leq T} \Sigma_t.$$

Thus A_T is the largest positive entropy-production excursion and B_T is the magnitude of the largest negative entropy-production excursion over the observation time. The pair (A_T, B_T) records more than the final entropy production. It records how far the trajectory wandered in both thermodynamic directions before it ended. Equivalently, each trajectory creates a path-dependent interval $[L_T, H_T]$ inside which the final martingale value M_T must lie. The upper-bound problem is therefore not only a problem about the endpoint distribution. It is also a problem about how terminal entropy production is placed inside intervals generated by the path.

First, positive entropy-production extrema alone are not enough. A bound on A_T alone cannot yield a non-trivial upper bound on $\langle \Sigma_T \rangle$. If $A_T \leq a$, then of course $\Sigma_T \leq a$ and hence $\langle \Sigma_T \rangle \leq a$. But this bound cannot be improved without additional information. A process can have Σ_T close to a with probability arbitrarily close to one, while the fluctuation relation is satisfied by extremely rare trajectories with very negative entropy production. In this sense, positive entropy-production extrema alone do not control the upper-bound side of the second law. The negative branch is not a technical nuisance; it is the mechanism by which the fluctuation relation balances large positive entropy production.

A nontrivial deterministic upper bound appears when both sides of the entropy-production range are controlled. If $-b \leq \Sigma_T \leq a$, or equivalently $e^{-a} \leq M_T \leq e^b$, convexity gives

$$\langle \Sigma_T \rangle \leq U(a, b) = \frac{a(e^b - 1) - b(1 - e^{-a})}{e^b - e^{-a}}.$$

This is the deterministic two-sided extrema bound later derived in Sec. III B, obtained by the secant line of $-\ln x$ over the interval $[e^{-a}, e^b]$. It is sharp, with equality for a two-point terminal distribution, or pathwise for a martingale stopped at the two corresponding barriers. In the limit $b \rightarrow \infty$, the bound reduces to the trivial one-sided value a , expressing again that unbounded negative entropy fluctuations can carry the exponential weight required by the fluctuation theorem.

The main contribution of this paper is to go beyond deterministic endpoint support and derive an upper envelope from the random path extrema (L_T, H_T) themselves. For each realized envelope $[L_T, H_T]$, the terminal value

M_T lies inside the interval. The convexity of $-\ln M_T$ gives an envelope-conditioned secant bound. If only the joint law of (L_T, H_T) is retained, the corresponding static relaxation becomes an allocation problem. Moving terminal weight from H_T to L_T increases entropy production, because $L_T = e^{-A_T}$ is the positive entropy-production end of the interval. But this move also changes the martingale mean and therefore consumes part of the normalization budget imposed by $\langle M_T \rangle = 1$. Different realized intervals give different entropy gains for the same martingale cost. The optimal relaxed bound is obtained by spending this budget first on the most efficient intervals.

This budget-allocation problem is mathematically a continuous knapsack problem. In the resulting relaxation, the relevant sorting variable is the entropy gain per martingale cost,

$$\rho(L_T, H_T) = \frac{\ln(H_T/L_T)}{H_T - L_T},$$

or, in entropy variables,

$$\rho(A_T, B_T) = \frac{A_T + B_T}{e^{B_T} - e^{-A_T}}.$$

This ratio is the entropy span per martingale cost of shifting terminal weight from H_T to L_T .

The resulting path-extrema upper envelope will be denoted \mathcal{U}_{ext} . It is not, in general, a dynamically attainable martingale optimum. A real martingale cannot freely rearrange terminal values inside realized envelopes, because the envelope is created by the path itself. There are then only two possible ways to fall below the relaxed envelope: the terminal value can sit inside its own realized interval, or the ensemble can place entropy-producing endings in less efficient envelope classes. Accordingly, the relation between the upper envelope and the actual mean entropy production is captured by an exact decomposition,

$$\langle \Sigma_T \rangle = \mathcal{U}_{\text{ext}} - \mathcal{A} - \mathcal{C}.$$

The term $\mathcal{A} \geq 0$ is an allocation gap across envelope classes. It measures the difference between the optimal envelope allocation and the actual conditional allocation of terminal values across different realized envelope classes. The term $\mathcal{C} \geq 0$ is a curvature gap within realized envelopes. It measures the curvature loss incurred when M_T lies inside its realized interval $[L_T, H_T]$ rather than at one of its endpoints. Thus the random path extrema define an upper envelope, while the dynamics determine how much of that envelope is actually reached.

This decomposition is the central result of the paper. It separates three distinct ideas that are conflated in a simple support bound. First, the running extrema determine the largest mean entropy production compatible with the envelope information and the fluctuation-theorem normalization. Second, the terminal value may fail to use the realized extrema because it lies in the interior of its path-defined interval. Third, even when terminal values lie at extrema, the ensemble may allocate

entropy-producing endings across envelope classes in a nonextremal way. The gap between the path-extrema upper envelope and the actual mean entropy production is exactly the sum of these two nonnegative contributions.

The paper is organized as follows. Section II sets up the entropy-production martingale, path extrema, and assumptions. Section III shows why positive extrema alone are not enough and proves the deterministic two-sided extrema bound. Section IV derives the random path-extrema upper envelope and its knapsack form. Section V proves the gap decomposition. Section VI presents four examples: a single-shot entropy fluctuation saturating the envelope, a mixture of operating modes with pure allocation gap, a two-stage martingale tree exhibiting both allocation and curvature gaps, and a concrete Markov-jump realization with local detailed balance.

II. ENTROPY-PRODUCTION MARTINGALE AND PATH EXTREMA

Let Σ_t denote the total stochastic entropy production accumulated up to time t . We focus on settings in which the exponential entropy production

$$M_t = e^{-\Sigma_t}$$

is a positive martingale with respect to the natural filtration of the process, i.e., the information contained in the trajectory up to time t . Thus $M_t > 0$, $M_0 = 1$, and $\langle M_T \rangle = 1$. The last relation is the integral fluctuation theorem at time T , $\langle e^{-\Sigma_T} \rangle = 1$. The full martingale property is stronger than the fixed-time fluctuation theorem and is needed when path extrema over the interval $[0, T]$ are used. Some of the endpoint support bounds below require only the fixed-time relation, while the path-extrema results use the martingale setting.

We define the running lower and upper extrema of M_t by

$$L_T = \inf_{0 \leq t \leq T} M_t, \quad H_T = \sup_{0 \leq t \leq T} M_t.$$

Since $M_0 = 1$, we have $L_T \leq 1 \leq H_T$ almost surely. The corresponding entropy-production extrema are

$$A_T = -\ln L_T = \sup_{0 \leq t \leq T} \Sigma_t, \quad B_T = \ln H_T = -\inf_{0 \leq t \leq T} \Sigma_t.$$

Thus A_T is the largest positive entropy production reached by the trajectory and B_T is the magnitude of the largest negative entropy production reached by the trajectory.

The terminal value M_T always lies inside its own realized envelope: $L_T \leq M_T \leq H_T$. Equivalently, $-B_T \leq \Sigma_T \leq A_T$. Figure 1 illustrates these three pieces separately: the entropy-production extrema in panel (a), the martingale envelope in panel (b), and the secant interpretation of the convexity bound in panel (c). The distinction between terminal support and path extrema will

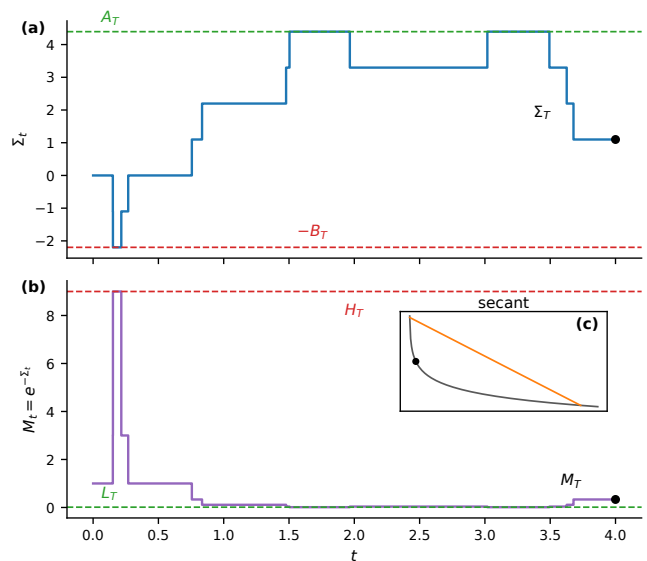


FIG. 1. Trajectory geometry for the entropy-production martingale. Panel (a) shows a sample entropy-production trajectory Σ_t , with the largest positive excursion A_T and the largest negative excursion $-B_T$. Panel (b) shows the corresponding exponential process $M_t = e^{-\Sigma_t}$, whose running minimum and maximum define the realized martingale envelope $[L_T, H_T]$; the terminal value M_T lies inside this interval. Panel (c) shows the local convexity geometry: for a fixed envelope, the convex function $-\ln m$ is bounded above by the secant joining $(L_T, -\ln L_T)$ and $(H_T, -\ln H_T)$. This secant construction represents the conditional terminal mean by an effective endpoint mixture on the martingale envelope.

be important. A deterministic support condition such as $e^{-a} \leq M_T \leq e^b$ constrains only the final value. By contrast, the random pair (L_T, H_T) records the actual lower and upper extrema reached along each path before the terminal time. The latter contains strictly more path information, but it also obeys additional dynamical constraints because the extrema are created by the martingale path itself.

Throughout the main text we assume $0 < L_T \leq M_T \leq H_T < \infty$ almost surely and that all logarithmic expectations appearing below are finite. In particular, we assume

$$\langle |\ln M_T| \rangle < \infty, \quad \langle |\ln L_T| \rangle < \infty, \quad \langle |\ln H_T| \rangle < \infty.$$

For the random-envelope upper bound we also assume $\langle H_T \rangle < \infty$. These assumptions can be weakened in standard ways by truncation, but they keep the presentation focused on the main mechanism.

On the event $L_T = H_T$, the martingale is constant over the interval and $M_T = L_T = H_T$. Such paths contribute no interval width. Whenever a ratio involving $H_T - L_T$ appears below, it is understood to be evaluated on the event $L_T < H_T$, with zero contribution assigned on $L_T = H_T$.

It will be useful to condition directly on the realized envelope (L_T, H_T) . Define the conditional terminal mean

by

$$\mu_T = \mathbb{E}[M_T | L_T, H_T].$$

Since $L_T \leq M_T \leq H_T$, it follows that $L_T \leq \mu_T \leq H_T$. We then define the envelope-conditioned endpoint weight

$$r_T = \frac{H_T - \mu_T}{H_T - L_T}. \quad (1)$$

This quantity satisfies $0 \leq r_T \leq 1$ and is the unique number for which $\mu_T = r_T L_T + (1 - r_T) H_T$. Thus r_T is the effective conditional weight that would reproduce the same conditional terminal mean by placing mass only at the two endpoints L_T and H_T .

The martingale normalization imposes a global constraint on r_T . Taking the expectation of the previous relation gives

$$1 = \langle M_T \rangle = \langle \mu_T \rangle = \langle r_T L_T + (1 - r_T) H_T \rangle.$$

Equivalently,

$$\langle r_T (H_T - L_T) \rangle = \langle H_T \rangle - 1. \quad (2)$$

This identity will be the constraint behind the path-extrema upper envelope. It expresses the amount by which terminal weight must be shifted from the upper endpoint H_T toward the lower endpoint L_T in order to satisfy $\langle M_T \rangle = 1$.

The entropy-production interpretation of r_T is direct. The endpoint $L_T = e^{-A_T}$ corresponds to the positive entropy-production extreme $\Sigma = A_T$, while $H_T = e^{B_T}$ corresponds to the negative entropy-production extreme $\Sigma = -B_T$. A larger value of r_T means that, conditional on the realized envelope, the terminal value is biased more strongly toward the entropy-producing endpoint.

We will also use the secant line of the convex function $f(m) = -\ln m$ over the interval $[L_T, H_T]$:

$$\ell_{L_T, H_T}(m) = \frac{H_T - m}{H_T - L_T} (-\ln L_T) + \frac{m - L_T}{H_T - L_T} (-\ln H_T).$$

For $m \in [L_T, H_T]$, convexity gives $-\ln m \leq \ell_{L_T, H_T}(m)$. This elementary inequality is the local building block of all the upper bounds below.

III. POSITIVE EXTREMA ARE NOT ENOUGH: DETERMINISTIC TWO-SIDED BOUND

Before treating random path extrema, it is useful to separate two simpler facts. The first shows that positive entropy-production extrema alone cannot give a nontrivial upper bound. The second is the deterministic two-sided bound obtained when both positive and negative entropy-production ranges are controlled.

A. The one-sided ceiling

Suppose that the positive entropy-production maximum is bounded by a deterministic value $a > 0$: $A_T = \sup_{0 \leq t \leq T} \Sigma_t \leq a$. Then, trivially, $\Sigma_T \leq A_T \leq a$, and hence $\langle \Sigma_T \rangle \leq a$. The important point is that no universal improvement below a is possible.

To see this, let $\ell = e^{-a}$ and consider, for $0 < \varepsilon < 1$, a one-step positive martingale with terminal value

$$M_T = \begin{cases} \ell, & \text{with probability } 1 - \varepsilon, \\ R_\varepsilon, & \text{with probability } \varepsilon. \end{cases}$$

The martingale condition $\langle M_T \rangle = 1$ fixes

$$R_\varepsilon = \frac{1 - (1 - \varepsilon)e^{-a}}{\varepsilon}.$$

The corresponding entropy production is

$$\Sigma_T = \begin{cases} a, & \text{with probability } 1 - \varepsilon, \\ -\ln R_\varepsilon, & \text{with probability } \varepsilon. \end{cases}$$

The positive maximum is bounded by a , while the mean entropy production is

$$\langle \Sigma_T \rangle = (1 - \varepsilon)a - \varepsilon \ln R_\varepsilon.$$

As $\varepsilon \rightarrow 0$, $R_\varepsilon \sim (1 - e^{-a})/\varepsilon$, so $\varepsilon \ln R_\varepsilon \rightarrow 0$ and therefore $\langle \Sigma_T \rangle \rightarrow a$. Thus $\sup\{\langle \Sigma_T \rangle : A_T \leq a\} = a$. This proves optimality for deterministic upper bounds that depend only on the ceiling $A_T \leq a$, not optimality relative to richer information such as the full law of A_T .

This construction shows why one-sided information is insufficient. The process can produce entropy close to a on almost every trajectory, while the fluctuation relation is maintained by extremely rare trajectories with very negative entropy production. The positive entropy-production ceiling does not control the exponential weight carried by the negative branch.

B. Deterministic two-sided bound

A nontrivial upper bound appears once both sides of the entropy-production range are controlled. Suppose $-b \leq \Sigma_T \leq a$ for deterministic $a, b > 0$. Equivalently, $e^{-a} \leq M_T \leq e^b$. The fixed-time fluctuation theorem gives $\langle M_T \rangle = 1$.

Let $f(m) = -\ln m$. On the interval $[e^{-a}, e^b]$, the convex function f lies below its secant line through the endpoint values (e^{-a}, a) and $(e^b, -b)$. Denote this deterministic secant line by $s_{a,b}(m)$, reserving $\ell_{L,H}(m)$ for secants written directly in martingale endpoints. Then $-\ln M_T \leq s_{a,b}(M_T)$, and taking expectations with $\langle M_T \rangle = 1$ gives

$$\langle \Sigma_T \rangle = \langle -\ln M_T \rangle \leq s_{a,b}(\langle M_T \rangle) = s_{a,b}(1).$$

A direct calculation yields

$$\begin{aligned} \langle \Sigma_T \rangle &\leq U(a, b) = \frac{a(e^b - 1) - b(1 - e^{-a})}{e^b - e^{-a}} \\ &= a - (a + b) \frac{e^a - 1}{e^{a+b} - 1}. \end{aligned} \quad (3)$$

The bound is sharp. Let

$$M_T = \begin{cases} e^{-a}, & \text{with probability } p, \\ e^b, & \text{with probability } 1 - p. \end{cases}$$

The condition $\langle M_T \rangle = 1$ gives $p = (e^b - 1)/(e^b - e^{-a})$. Then

$$\Sigma_T = \begin{cases} a, & \text{with probability } p, \\ -b, & \text{with probability } 1 - p, \end{cases}$$

and the mean entropy production equals $U(a, b)$. Pathwise, the same equality case can be realized by a martingale stopped when it first reaches either e^{-a} or e^b .

The limit $b \rightarrow \infty$ recovers the one-sided result: $U(a, b) \rightarrow a$. Thus the nontrivial part of the upper bound comes from controlling the negative entropy-production side. If arbitrarily negative entropy-production trajectories are allowed, the fluctuation relation can be satisfied by events of vanishing probability but arbitrarily large exponential weight.

It is important to distinguish the deterministic support bound in Eq. (3) from the path-extrema bounds developed below. The condition $e^{-a} \leq M_T \leq e^b$ constrains the endpoint distribution. It does not imply that each trajectory realizes both extrema along its path. A martingale stopped at the two barriers, for example, hits only one of the two barriers on each path. The random path-extrema problem keeps track of the realized interval $[L_T, H_T]$ for each trajectory and therefore contains additional path information.

IV. RANDOM PATH-EXTREMA UPPER ENVELOPE

We now turn from deterministic endpoint support to the random path extrema themselves. For each trajectory, the terminal martingale value lies inside its realized interval, $L_T \leq M_T \leq H_T$. The random pair (L_T, H_T) records how far that particular path moved in the entropy-producing and entropy-consuming directions before time T . The key point is that these intervals are random: different trajectories create different available ranges for the terminal value. We first derive a bound after conditioning on one realized envelope, and then ask what upper bound remains if only the statistics of the realized envelopes are kept.

A. Envelope-conditioned secant bound

Condition on the realized envelope (L_T, H_T) and use the endpoint weight r_T defined in Eq. (1). For fixed L_T and H_T , the only remaining random variable is the terminal point M_T inside the interval. Convexity of $-\ln m$ gives the secant inequality

$$\begin{aligned} -\ln m &\leq \ell_{L_T, H_T}(m) \\ &= \frac{H_T - m}{H_T - L_T}(-\ln L_T) + \frac{m - L_T}{H_T - L_T}(-\ln H_T) \end{aligned}$$

for all $m \in [L_T, H_T]$.

We now apply this inequality inside a fixed realized envelope. Taking the conditional expectation over M_T while holding (L_T, H_T) fixed gives

$$\mathbb{E}[-\ln M_T \mid L_T, H_T] \leq -\ln H_T + r_T \ln \frac{H_T}{L_T}. \quad (4)$$

Here the endpoint weight r_T enters because the conditional mean of M_T is $\mu_T = r_T L_T + (1 - r_T) H_T$.

Finally, averaging Eq. (4) over the realized envelopes gives

$$\langle \Sigma_T \rangle \leq \mathcal{U}_{\text{cond}}, \quad (5)$$

where

$$\mathcal{U}_{\text{cond}} = \langle -\ln H_T \rangle + \left\langle r_T \ln \frac{H_T}{L_T} \right\rangle. \quad (6)$$

Thus $\mathcal{U}_{\text{cond}}$ is the upper bound obtained when the actual conditional endpoint weight r_T is still known. This is still a bound for the actual process, because it uses the actual conditional mean μ_T , encoded in r_T . If this conditional information is removed, the individual endpoint weights are unknown. What remains is only their total martingale cost, fixed by Eq. (2). The next step therefore turns the problem into one of distributing this cost across realized envelopes.

In entropy variables, $L_T = e^{-A_T}$ and $H_T = e^{B_T}$, so $-\ln H_T = -B_T$ and $\ln(H_T/L_T) = A_T + B_T$. Thus

$$\mathcal{U}_{\text{cond}} = -\langle B_T \rangle + \langle r_T(A_T + B_T) \rangle.$$

The weight r_T measures the effective conditional bias toward the positive entropy-production endpoint A_T .

B. Static upper envelope and knapsack form

Suppose now that only the joint law of (L_T, H_T) is retained, while the conditional terminal mean inside each envelope is discarded. We then no longer know the actual function r_T . What remains is the global martingale-normalization constraint. The actual r_T is one such function, since it satisfies the martingale-cost constraint in Eq. (2). To obtain the largest mean entropy production compatible with the retained envelope statistics, we relax

the dynamics and optimize over all envelope-dependent weight functions $r(L_T, H_T)$ with $0 \leq r \leq 1$ satisfying the same global constraint. Starting from the actual-process bound $\mathcal{U}_{\text{cond}}$, we keep the same envelope-dependent payoff but replace the unknown actual weight r_T by the best weight function r allowed by the martingale normalization.

We define the path-extrema upper envelope

$$\begin{aligned} \mathcal{U}_{\text{ext}} = & \langle -\ln H_T \rangle \\ & + \sup_{0 \leq r \leq 1} \left\{ \left\langle r \ln \frac{H_T}{L_T} \right\rangle : \langle r(H_T - L_T) \rangle = \langle H_T \rangle - 1 \right\}. \end{aligned} \quad (7)$$

This is a static relaxation: it treats the endpoint placement inside each realized envelope as a choice variable, while keeping the envelope statistics and the martingale normalization fixed. Since the actual r_T satisfies the same constraint, the preceding bound immediately implies $\langle \Sigma_T \rangle \leq \mathcal{U}_{\text{ext}}$. This gives a universal static upper bound determined by the path-extrema statistics.

The constraint in Eq. (7) is always feasible. Since $L_T \leq M_T \leq H_T$ and $\langle M_T \rangle = 1$, $\langle L_T \rangle \leq 1 \leq \langle H_T \rangle$. Therefore $0 \leq \langle H_T \rangle - 1 \leq \langle H_T - L_T \rangle$. Hence there exists at least one envelope-dependent weight function $r \in [0, 1]$ satisfying the constraint. The actual conditional weight r_T is one such function.

The variational problem in Eq. (7) is linear. Let

$$c_T = \ln \frac{H_T}{L_T}, \quad d_T = H_T - L_T, \quad K = \langle H_T \rangle - 1.$$

Then the optimization is

$$\sup_{0 \leq r \leq 1} \langle r c_T \rangle$$

subject to

$$\langle r d_T \rangle = K.$$

This is a continuous knapsack problem with a direct physical interpretation. Each value, or empirical bin, of the realized envelope (L_T, H_T) has a limited ‘‘cost’’ d_T for moving terminal weight from H_T to L_T , and a corresponding entropy ‘‘gain’’ c_T . Choosing $r = 1$ on a given envelope class places the terminal value, in the relaxed problem, at the lower martingale endpoint L_T , corresponding to the positive entropy-production endpoint A_T . Choosing $r = 0$ places it at the upper martingale endpoint H_T , corresponding to the negative entropy-production endpoint $-B_T$.

The gain from choosing L_T rather than H_T is $c_T = \ln(H_T/L_T)$, while the martingale cost is $d_T = H_T - L_T$. Thus the relevant efficiency ratio is

$$\rho_T = \frac{\ln(H_T/L_T)}{H_T - L_T}. \quad (8)$$

Figure 2 summarizes this construction by showing the realized envelope classes in cost-gain coordinates, the selected classes, and the possible threshold class in the

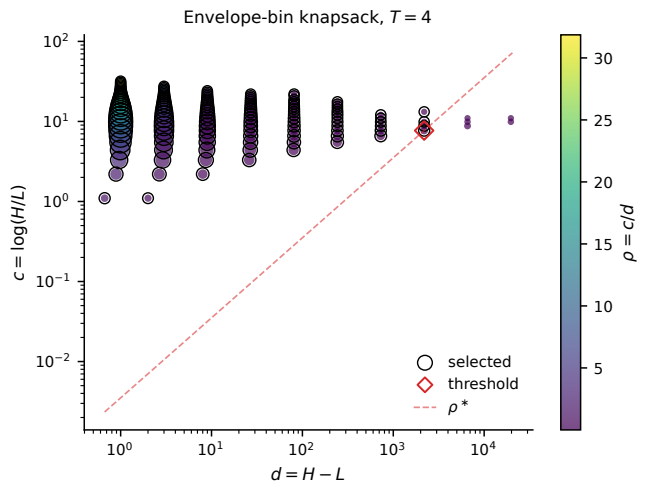


FIG. 2. Empirical envelope classes for the random path-extrema optimization. Each point represents a realized envelope class in cost-gain coordinates (d, c) , where moving terminal weight from H to L gives entropy gain $c = \ln(H/L)$ and consumes martingale cost $d = H - L$. Classes are ranked by $\rho = c/d$. The selected classes fill the martingale-cost budget in decreasing order of ρ , with a possible fractional threshold class at the boundary.

fractional-knapsack rule. In entropy variables, $\rho_T = (A_T + B_T)/(e^{B_T} - e^{-A_T})$. The one-sided limits are

$$\rho(A, 0) = \frac{A}{1 - e^{-A}}, \quad \rho(0, B) = \frac{B}{e^B - 1},$$

and $\rho(A, B) \rightarrow 1$ as $A, B \rightarrow 0$. For fixed B , $\rho(A, B)$ increases with A ; for fixed A , it decreases with B . The optimal weight function assigns $r = 1$ first to envelope classes with the largest ρ_T , then to classes with progressively smaller ρ_T , with possible partial assignment at one threshold.

More explicitly, an optimal weight function r_T^* has the threshold form

$$r_T^* = \begin{cases} 1, & \rho_T > \lambda, \\ 0, & \rho_T < \lambda, \\ \theta_T \in [0, 1], & \rho_T = \lambda, \end{cases}$$

where λ and θ_T are chosen so that

$$\langle r_T^*(H_T - L_T) \rangle = \langle H_T \rangle - 1.$$

If a nonzero fraction of envelope classes has exactly the threshold value $\rho_T = \lambda$, the optimal weight function r_T^* need not be unique. However, all choices that satisfy the same budget have the same objective value, so \mathcal{U}_{ext} and \mathcal{A} are independent of the tie-breaking convention. Equivalently, if $\rho^*(u)$ denotes the decreasing rearrangement of ρ_T with respect to the measure $d\nu = (H_T - L_T)d\mathbb{P}$, meaning that envelope classes are listed from largest to smallest efficiency while weighted by their martingale cost,

then

$$\mathcal{U}_{\text{ext}} = \langle -\ln H_T \rangle + \int_0^{\langle H_T \rangle^{-1}} \rho^*(u) du.$$

This form emphasizes that the upper envelope is determined by ranking envelope classes according to entropy span per martingale cost.

The path-extrema upper envelope is therefore an upper envelope, not automatically a dynamically attainable martingale optimum. Equation (7) allows the endpoint assignment r_T^* to be chosen after the envelope class is known. A real martingale has less freedom: the envelope is produced by the path, and the terminal value is coupled to the history that created that envelope. These dynamical constraints are not captured by the static optimization. The next section shows that the difference between the static upper envelope and the actual mean entropy production can nevertheless be written exactly as the sum of two nonnegative gap terms.

V. GAP DECOMPOSITION

The upper envelope \mathcal{U}_{ext} is obtained by relaxing the actual martingale dynamics to an optimal allocation problem over the realized path-extrema classes. A real martingale need not attain this envelope. In this section we show that the difference between the envelope and the actual mean entropy production has an exact decomposition into two nonnegative gap terms.

Let r_T^* denote an optimal weight function for the static problem in Eq. (7), that is, a choice of r that attains the supremum. The actual process has the envelope-conditioned weight r_T defined in Eq. (1). Both r_T and r_T^* satisfy the same martingale-cost constraint, $\langle r(H_T - L_T) \rangle = \langle H_T \rangle - 1$.

We define the cross-envelope allocation gap by

$$\mathcal{A} = \left\langle (r_T^* - r_T) \ln \frac{H_T}{L_T} \right\rangle. \quad (9)$$

Because r_T^* maximizes the linear functional in Eq. (7) and r_T satisfies the same constraint, we have $\mathcal{A} \geq 0$. This term measures the gap from using the actual allocation r_T rather than the envelope-optimal allocation r_T^* across different realized path-extrema classes.

Next define the within-envelope curvature gap using the secant line ℓ_{L_T, H_T} defined in Sec. II:

$$\mathcal{C} = \langle \ell_{L_T, H_T}(M_T) - (-\ln M_T) \rangle. \quad (10)$$

Convexity of $-\ln m$ gives $\mathcal{C} \geq 0$. This term measures the curvature loss from terminal values lying inside their realized intervals rather than at one of the two endpoints.

We now combine the definitions. By the definition of the static upper envelope and the optimal weight function r_T^* ,

$$\mathcal{U}_{\text{ext}} = \langle -\ln H_T \rangle + \left\langle r_T^* \ln \frac{H_T}{L_T} \right\rangle. \quad (11)$$

The actual conditional bound in Eq. (6) is

$$\mathcal{U}_{\text{cond}} = \langle -\ln H_T \rangle + \left\langle r_T \ln \frac{H_T}{L_T} \right\rangle. \quad (12)$$

Subtracting Eq. (12) from Eq. (11) and using the definition of \mathcal{A} in Eq. (9) gives

$$\mathcal{U}_{\text{ext}} - \mathcal{U}_{\text{cond}} = \mathcal{A}. \quad (13)$$

On the other hand, the envelope-conditioned secant construction gives

$$\langle \ell_{L_T, H_T}(M_T) \rangle = \mathcal{U}_{\text{cond}}, \quad (14)$$

so the definition of \mathcal{C} in Eq. (10) gives

$$\mathcal{U}_{\text{cond}} - \langle \Sigma_T \rangle = \mathcal{C}. \quad (15)$$

Finally, combining Eqs. (13) and (15) yields the central identity

$$\langle \Sigma_T \rangle = \mathcal{U}_{\text{ext}} - \mathcal{A} - \mathcal{C}. \quad (16)$$

Equation (16) is the path-extrema gap decomposition. The first term, \mathcal{U}_{ext} , is the static upper envelope determined by the statistics of the running extrema and the martingale normalization. The term \mathcal{A} is a cross-envelope allocation gap, while \mathcal{C} is a within-envelope curvature gap.

Physically, the decomposition separates two ways in which a real process can fall below the relaxed path-extrema envelope. The allocation gap \mathcal{A} is an ensemble-level penalty: entropy-producing terminal outcomes may occur in envelope classes that are not the most efficient ones according to ρ_T . The curvature gap \mathcal{C} is a trajectory-level terminal-placement penalty: after a path has created an interval $[L_T, H_T]$, the terminal value may end in the interior rather than at an endpoint. Thus \mathcal{U}_{ext} measures the best static use of the observed path-extrema statistics, while \mathcal{A} and \mathcal{C} identify how the actual dynamics fail to use that envelope optimally.

Although Eq. (16) is algebraically telescopic once $\mathcal{U}_{\text{cond}}$ is introduced, the split is not arbitrary. The conditioned secant bound $\mathcal{U}_{\text{cond}}$ is the natural intermediate object obtained by first fixing the realized envelope and applying the local convexity bound. It separates the local curvature gap inside each envelope from the global allocation gap produced when the actual endpoint weights differ from the knapsack allocation.

The equality conditions are immediate. On the event $L_T = H_T$ the condition is satisfied trivially; on its complement, $\mathcal{C} = 0$ requires M_T to equal one of the two endpoints almost surely. The allocation gap vanishes if and only if the actual envelope-conditioned weight r_T is an optimal weight function for the static problem in Eq. (7). Thus the upper envelope is attained exactly when terminal values lie at realized extrema and the endpoint allocation across envelope classes is extremal.

It is useful to make the curvature gap more quantitative. Since $f(m) = -\ln m$ satisfies $f''(m) = 1/m^2$, for $m \in [L_T, H_T]$ we have

$$\frac{1}{H_T^2} \leq f''(m) \leq \frac{1}{L_T^2}.$$

The interpolation error for a twice differentiable convex function gives

$$\begin{aligned} \frac{(H_T - m)(m - L_T)}{2H_T^2} &\leq \ell_{L_T, H_T}(m) - f(m) \\ &\leq \frac{(H_T - m)(m - L_T)}{2L_T^2}. \end{aligned}$$

Therefore

$$\mathcal{C} \geq \left\langle \frac{(H_T - M_T)(M_T - L_T)}{2H_T^2} \right\rangle.$$

When the upper expectation is finite, one also has

$$\mathcal{C} \leq \left\langle \frac{(H_T - M_T)(M_T - L_T)}{2L_T^2} \right\rangle.$$

This lower bound shows explicitly that terminal values in the interior of their realized path-extrema intervals force a positive gap below the upper envelope.

The decomposition in Eq. (16) also clarifies why universal dynamic sharpness of \mathcal{U}_{ext} should not be assumed. The optimization defining \mathcal{U}_{ext} treats each realized interval $[L_T, H_T]$ as if the terminal endpoint allocation could be chosen freely, subject only to the global martingale normalization. In an actual martingale, however, the envelope is produced by the path. The order in which the path reaches its extrema and the optional-stopping constraints of the martingale restrict how terminal values can be coupled to (L_T, H_T) . These restrictions appear in Eq. (16) as nonzero gap terms.

VI. EXAMPLES

We now illustrate the decomposition in Eq. (16). The first three examples are deliberately simple martingale constructions. They isolate the mathematical mechanisms behind saturation, allocation gap, and curvature gap. The final example gives a concrete stochastic-thermodynamic realization in a continuous-time Markov jump process with local detailed balance.

A. Single-shot entropy fluctuation: saturation of the envelope

Consider a one-step positive martingale with $M_0 = 1$ and $M_T = Z$, where $Z > 0$ and $\langle Z \rangle = 1$. This is the minimal fixed-time representation of an entropy-production fluctuation satisfying the integral fluctuation theorem:

$\Sigma_T = -\ln Z$ and $\langle e^{-\Sigma_T} \rangle = \langle Z \rangle = 1$. This example represents a single-shot entropy-production measurement in which no intermediate time information is retained. It may be viewed as an effective description of a short experiment, a coarse-grained transition record, or a two-outcome entropy measurement. It is not yet a full continuous-time stochastic-thermodynamic model, because it keeps only the fixed-time entropy fluctuation and discards the dynamical path by which it was produced.

For this one-step process, $L_T = \min(1, Z)$ and $H_T = \max(1, Z)$. In this degenerate one-step path, the only possible extrema are the initial value and the terminal value. Thus M_T always lies at one of the two endpoints of its realized envelope: $M_T \in \{L_T, H_T\}$. Therefore the curvature gap vanishes, $\mathcal{C} = 0$.

The allocation gap also vanishes. If $Z < 1$, then $M_T = L_T$ and $H_T = 1$. The corresponding efficiency ratio is

$$\rho_T = \frac{\ln(1/Z)}{1 - Z} > 1.$$

If $Z > 1$, then $M_T = H_T$ and $L_T = 1$, and

$$\rho_T = \frac{\ln Z}{Z - 1} < 1.$$

Hence the actual endpoint assignment is a threshold rule in ρ_T : entropy-producing terminal outcomes occupy the high- ρ_T classes, while entropy-consuming terminal outcomes occupy the low- ρ_T classes. This is precisely the optimizer of the knapsack problem. Thus $\mathcal{A} = 0$. Equation (16) gives $\langle \Sigma_T \rangle = \mathcal{U}_{\text{ext}}$ for every one-step martingale.

This example is useful as an equality benchmark. When the entropy-production record has no internal temporal structure, the terminal value necessarily coincides with a realized path extremum, and the path-extrema upper envelope is saturated.

B. Mixture of operating modes: pure allocation gap

The second example isolates the allocation gap \mathcal{A} . Consider an ensemble in which, before each run, a device is placed in one of two operating modes. Each mode has its own entropy-production window. Conditional on the mode, the terminal value lies at one of the two endpoints of that window, so there is no within-envelope curvature gap. The only possible gap is the allocation of entropy-producing endings across the two modes.

This example should be interpreted as a static envelope-allocation example, or support-window relaxation, rather than as a claim that a continuous-time martingale realizes exactly the specified joint law of (L_T, H_T, M_T) . Its role is to isolate \mathcal{A} with $\mathcal{C} = 0$.

Let the two modes occur with probabilities 1/2 and 1/2. In mode 1, set

$$L_1 = \frac{1}{2}, \quad H_1 = \frac{3}{2}.$$

In mode 2, set

$$L_2 = \frac{1}{5}, \quad H_2 = 5.$$

Within each mode, let $M_T \in \{L_j, H_j\}$ with conditional probability r_j of ending at L_j . We choose r_j so that the conditional mean is one: $r_j L_j + (1 - r_j) H_j = 1$. Thus $r_j = (H_j - 1)/(H_j - L_j)$. For the two modes, $r_1 = \frac{1}{2}$ and $r_2 = \frac{5}{6}$. Each mode separately satisfies $\mathbb{E}[M_T | j] = 1$, and therefore the full ensemble satisfies $\langle M_T \rangle = 1$.

The mean entropy production is

$$\langle \Sigma_T \rangle = \frac{1}{2} \left[\frac{1}{2} \ln 2 - \frac{1}{2} \ln \frac{3}{2} \right] + \frac{1}{2} \left[\frac{5}{6} \ln 5 - \frac{1}{6} \ln 5 \right].$$

Equivalently,

$$\langle \Sigma_T \rangle = \frac{1}{4} \ln \frac{4}{3} + \frac{1}{3} \ln 5.$$

Numerically, $\langle \Sigma_T \rangle \simeq 0.6084$.

The efficiency ratios of the two mode windows are

$$\rho_1 = \frac{\ln(H_1/L_1)}{H_1 - L_1} = \ln 3 \simeq 1.0986,$$

and

$$\rho_2 = \frac{\ln(H_2/L_2)}{H_2 - L_2} = \frac{\ln 25}{24/5} \simeq 0.6706.$$

Thus mode 1 is the more efficient envelope class in the sense of Eq. (8). The path-extrema upper envelope therefore assigns the entropy-producing endpoint first to mode 1.

The martingale-cost budget is

$$K = \langle H_T \rangle - 1 = \frac{1}{2} \cdot \frac{3}{2} + \frac{1}{2} \cdot 5 - 1 = \frac{9}{4}.$$

The cost of assigning all mode-1 trajectories to the lower endpoint is

$$\frac{1}{2}(H_1 - L_1) = \frac{1}{2}.$$

Thus the optimal allocation sets

$$r_1^* = 1.$$

The remaining cost is $9/4 - 1/2 = 7/4$. Since the full mode-2 cost is

$$\frac{1}{2}(H_2 - L_2) = \frac{12}{5},$$

the optimal allocation uses

$$r_2^* = \frac{7/4}{12/5} = \frac{35}{48}.$$

Therefore

$$r_1^* = 1, \quad r_2^* = \frac{35}{48}.$$

The resulting upper envelope is

$$\mathcal{U}_{\text{ext}} = \langle -\ln H_T \rangle + \left\langle r_T^* \ln \frac{H_T}{L_T} \right\rangle,$$

which gives numerically

$$\mathcal{U}_{\text{ext}} \simeq 0.7154.$$

Since terminal values are always at endpoints, $\mathcal{C} = 0$. Hence the entire gap is the allocation gap:

$$\mathcal{A} = \mathcal{U}_{\text{ext}} - \langle \Sigma_T \rangle \simeq 0.1070.$$

This example shows that endpoint saturation alone does not guarantee saturation of the path-extrema upper envelope. Even when M_T always lies at L_T or H_T , the ensemble may place entropy-producing terminal outcomes in envelope classes that are not optimal according to the efficiency ratio ρ_T . In physical terms, two operating modes may each obey the fluctuation theorem, but the full ensemble can still fall below the extremal envelope because the entropy-producing outcomes are allocated inefficiently across modes.

C. Two-stage martingale tree: allocation and curvature gaps

The third example is a genuine multistep martingale. It shows both a cross-envelope allocation gap and a within-envelope curvature gap.

Let

$$M_0 = 1.$$

At the first step,

$$M_1 = \begin{cases} 1/2, & \text{with probability } 2/3, \\ 2, & \text{with probability } 1/3. \end{cases}$$

The mean is one:

$$\frac{2}{3} \cdot \frac{1}{2} + \frac{1}{3} \cdot 2 = 1.$$

At the second step, from $M_1 = 1/2$, set

$$M_2 = \begin{cases} 1/4, & \text{with probability } 1/2, \\ 3/4, & \text{with probability } 1/2. \end{cases}$$

The conditional mean is $1/2$. From $M_1 = 2$, set

$$M_2 = \begin{cases} 3/2, & \text{with probability } 2/3, \\ 3, & \text{with probability } 1/3. \end{cases}$$

The conditional mean is 2. Thus M_t is a positive martingale.

The four terminal paths are summarized in Table I.

TABLE I. Two-stage martingale tree. The terminal entropy production is $\Sigma_T = -\ln M_T$.

Path	Probability	M_T	L_T	H_T
$1 \rightarrow 1/2 \rightarrow 1/4$	1/3	1/4	1/4	1
$1 \rightarrow 1/2 \rightarrow 3/4$	1/3	3/4	1/2	1
$1 \rightarrow 2 \rightarrow 3/2$	2/9	3/2	1	2
$1 \rightarrow 2 \rightarrow 3$	1/9	3	1	3

For the four rows, the corresponding (Σ_T, ρ_T) values are $(\ln 4, 4 \ln 4/3)$, $(\ln(4/3), 2 \ln 2)$, $(-\ln(3/2), \ln 2)$, and $(-\ln 3, \ln 3/2)$.

The actual mean entropy production is

$$\langle \Sigma_T \rangle = \frac{1}{3} \ln 4 + \frac{1}{3} \ln \frac{4}{3} - \frac{2}{9} \ln \frac{3}{2} - \frac{1}{9} \ln 3.$$

Numerically,

$$\langle \Sigma_T \rangle \simeq 0.3458.$$

The efficiency ratios for the four realized envelopes are

(L_T, H_T)	ρ_T
(1/4, 1)	$\ln 4/(3/4) \simeq 1.8484$
(1/2, 1)	$\ln 2/(1/2) \simeq 1.3863$
(1, 2)	$\ln 2 \simeq 0.6931$
(1, 3)	$\ln 3/2 \simeq 0.5493$

The path-extrema upper envelope obtained from Eq. (7) is

$$\mathcal{U}_{\text{ext}} \simeq 0.4363.$$

The gap is therefore

$$\mathcal{U}_{\text{ext}} - \langle \Sigma_T \rangle \simeq 0.0905.$$

Using Eqs. (9) and (10), one finds

$$\mathcal{A} \simeq 0.0578, \quad \mathcal{C} \simeq 0.0327.$$

Thus

$$0.0905 \simeq 0.0578 + 0.0327,$$

as required by Eq. (16).

The origin of \mathcal{C} is visible directly from the tree. Two terminal paths end strictly inside their realized envelopes:

$$1 \rightarrow \frac{1}{2} \rightarrow \frac{3}{4}, \quad 1 \rightarrow 2 \rightarrow \frac{3}{2}.$$

For the first of these,

$$L_T = \frac{1}{2}, \quad M_T = \frac{3}{4}, \quad H_T = 1.$$

For the second,

$$L_T = 1, \quad M_T = \frac{3}{2}, \quad H_T = 2.$$

On these paths, $L_T < M_T < H_T$, so the secant inequality is strict. These paths generate the within-envelope curvature gap.

The allocation gap \mathcal{A} has a different origin. The relaxed upper envelope assigns entropy-producing endpoints according to the global efficiency ranking of the envelope classes. The actual two-stage martingale cannot freely rearrange its terminal endpoints after the first branching event. Its endpoint allocation is constrained by its temporal structure, and this produces the cross-envelope allocation gap.

This example can be read as a minimal two-stage nonequilibrium experiment. The first stage creates an entropy-producing or entropy-consuming fluctuation. The second stage either amplifies that fluctuation or partially relaxes it back toward neutrality. The trajectories that relax toward the interior do not use the full entropy interval they have created, giving $\mathcal{C} > 0$. The branching structure also prevents the ensemble from allocating entropy-producing endings across envelope classes in the extremal way, giving $\mathcal{A} > 0$.

D. Markov-jump realization with local detailed balance

We finally describe how the same quantities can be estimated in a genuine stochastic-thermodynamic model. Consider a continuous-time Markov jump process on three states arranged in a nonequilibrium cycle,

$$1 \rightleftharpoons 2 \rightleftharpoons 3 \rightleftharpoons 1.$$

Let k_{ij} denote the transition rate from state i to state j . Local detailed balance assigns to each jump $i \rightarrow j$ the medium entropy increment

$$\Delta s_{ij} = \ln \frac{k_{ij}}{k_{ji}}.$$

For a trajectory X_t observed in the nonequilibrium steady state π , the total entropy production over $[0, t]$ is

$$\Sigma_t = \ln \frac{\pi(X_0)}{\pi(X_t)} + \sum_{0 < \tau \leq t} \ln \frac{k_{X_\tau - X_\tau}}{k_{X_\tau X_\tau -}},$$

where the sum runs over jump times. In the steady state, $M_t = e^{-\Sigma_t}$ is the likelihood-ratio martingale between the forward trajectory measure and the time-reversed trajectory measure restricted to the observation interval. Therefore the path-extrema framework applies directly.

A minimal driven example is obtained by taking clockwise rates

$$k_{12} = k_{23} = k_{31} = k_+$$

and counterclockwise rates

$$k_{21} = k_{32} = k_{13} = k_-.$$

with $k_+ > k_-$. The steady state is uniform by symmetry, so the system-entropy boundary term vanishes and each clockwise jump contributes $\ln(k_+/k_-)$ while each counterclockwise jump contributes $-\ln(k_+/k_-)$. Thus

$$\Sigma_t = N_+(t) \ln \frac{k_+}{k_-} - N_-(t) \ln \frac{k_+}{k_-},$$

where $N_+(t)$ and $N_-(t)$ are the numbers of clockwise and counterclockwise jumps. Along each simulated trajectory one records

$$M_t = e^{-\Sigma_t}, \quad L_T = \inf_{0 \leq t \leq T} M_t, \quad H_T = \sup_{0 \leq t \leq T} M_t,$$

and then estimates $\langle \Sigma_T \rangle$, \mathcal{U}_{ext} , \mathcal{A} , and \mathcal{C} from the empirical ensemble.

This example makes the observables concrete. The extrema (L_T, H_T) are not auxiliary mathematical variables; they are obtained by monitoring the running maximum and minimum of the exponential entropy-production process along each trajectory. The conditional weight r_T can be estimated by binning trajectories with similar (L_T, H_T) and computing the conditional terminal mean $\mathbb{E}[M_T | L_T, H_T]$. The upper envelope \mathcal{U}_{ext} is then obtained by sorting the observed envelope classes by the empirical efficiency ratio

$$\rho_T = \frac{\ln(H_T/L_T)}{H_T - L_T}$$

and filling the martingale-cost budget $\langle H_T \rangle - 1$. In finite data, this is simply a weighted sorting problem.

The symmetric three-state cycle also clarifies the relation to long-time thermodynamics. The mean entropy production grows linearly at rate

$$\sigma = 3\pi_1 k_+ \ln \frac{k_+}{k_-} - 3\pi_1 k_- \ln \frac{k_+}{k_-} = (k_+ - k_-) \ln \frac{k_+}{k_-},$$

where $\pi_1 = 1/3$ in the symmetric steady state. The path-extrema envelope and the two gap terms may also grow with time, but their asymptotic rates need not coincide with σ . They depend on the rare negative fluctuations that determine H_T and on the frequency with which terminal values remain inside previously generated extrema. Thus the decomposition provides a way to ask whether the upper envelope, the allocation gap, and the curvature gap have separate large-time rates in a given physical process.

Figure 3 demonstrates this decomposition in a concrete physical Markov-jump simulation: panel (a) compares $\langle \Sigma_T \rangle$ with \mathcal{U}_{ext} , panel (b) resolves the two gap terms, and panel (c) shows the closure error.

VII. DISCUSSION

The results above give a path-extrema interpretation of upper bounds on mean entropy production. The central point is that the upper-bound side of the second

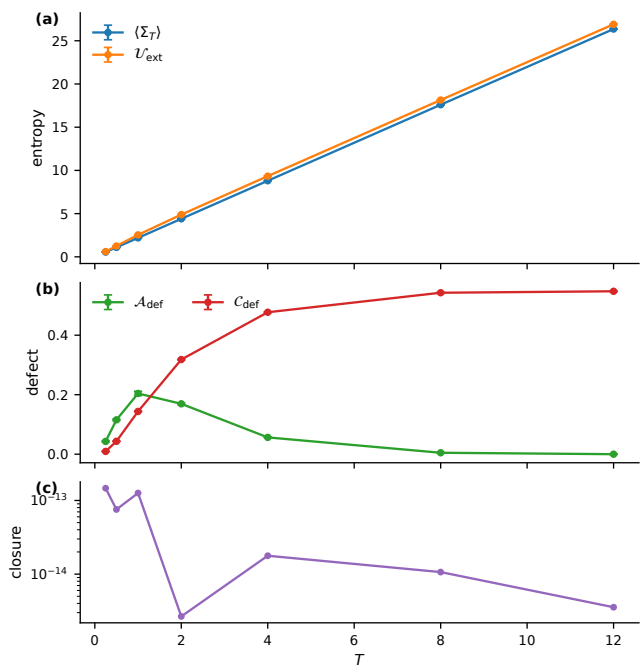


FIG. 3. Three-state Markov-jump realization of the path-extrema decomposition. Panel (a) compares the measured mean entropy production $\langle \Sigma_T \rangle$ with the empirical upper envelope \mathcal{U}_{ext} . Panel (b) shows the two nonnegative gap terms, the allocation gap \mathcal{A} and the curvature gap \mathcal{C} . Panel (c) reports the numerical closure error in the decomposition. Simulations use $k_+ = 3$, $k_- = 1$, 2×10^5 trajectories per T , 80×80 envelope bins, and 20 independent batches. At $T = 12$, the raw estimate $\mathcal{A}_{\text{raw}} = -5.74 \times 10^{-4}$ is within two batch standard errors of zero ($\text{SE} = 1.24 \times 10^{-3}$), so the plotted reported value is clipped to zero while the raw diagnostic remains in the summary table.

law is not controlled by the positive entropy-production maximum alone. A trajectory may reach large positive entropy production, but the fluctuation relation requires compensating negative entropy-production fluctuations. If those negative fluctuations are unconstrained, the compensation can be carried by events of arbitrarily small probability and arbitrarily large exponential weight. This is why a one-sided bound on $A_T = \sup_{0 \leq t \leq T} \Sigma_t$ gives no improvement over the trivial endpoint bound.

The deterministic two-sided result in Eq. (3) is the simplest nontrivial expression of this mechanism. If $-b \leq \Sigma_T \leq a$, then the fluctuation theorem and convexity of $-\ln M_T$ give the upper bound $U(a, b)$. This is the same secant-line structure underlying the extrema bound in Ref. [11]. The present work reframes that structure in a path-extrema martingale language and then extends it to random realized envelopes.

The random path-extrema bound is different from a deterministic support bound. The pair (L_T, H_T) records the actual running minimum and maximum of $M_t = e^{-\Sigma_t}$ along each trajectory. These extrema define, for each path, the interval in which the terminal value M_T lies.

If only the statistics of these intervals are retained, the largest compatible mean entropy production is described by the upper envelope \mathcal{U}_{ext} . Its variational form is a continuous knapsack problem. The efficiency ratio

$$\rho_T = \frac{\ln(H_T/L_T)}{H_T - L_T} = \frac{A_T + B_T}{e^{B_T} - e^{-A_T}}$$

ranks path-extrema classes by entropy span per martingale cost.

The upper envelope \mathcal{U}_{ext} should not be interpreted as a universally attainable martingale optimum. It is a static relaxation over the joint law of the realized intervals $[L_T, H_T]$. The static relaxation is allowed to decide, for each envelope class, how much terminal weight is placed at L_T rather than H_T , subject only to the global martingale normalization. A real martingale has less freedom. The envelope is itself generated by the path, and the terminal value must be coupled to the order and manner in which the extrema were reached. Equivalently, the optimizing allocation in Eq. (7) need not correspond to any realizable martingale coupling between terminal values and path-generated envelopes. This is the point at which the problem touches the general martingale-transport framework: one is not merely prescribing a terminal law, but asking which terminal-envelope couplings can be produced by a positive martingale with specified path extrema [21]. The exact gap decomposition in Eq. (16) is therefore the more physically meaningful statement:

$$\langle \Sigma_T \rangle = \mathcal{U}_{\text{ext}} - \mathcal{A} - \mathcal{C}.$$

The allocation gap \mathcal{A} measures the difference between the optimal cross-envelope allocation and the actual allocation produced by the dynamics. The curvature gap \mathcal{C} measures the gap caused by terminal values lying inside their realized extrema intervals. Thus the gap to the path-extrema envelope is not a single undifferentiated slack term; it has two distinct sources.

In short, \mathcal{C} is the price of ending inside an interval already created by the path, while \mathcal{A} is the price of using the available intervals in the wrong order.

This distinction clarifies the role of temporal structure. In a one-step entropy-production fluctuation, the terminal value is automatically an endpoint of its realized interval, and the allocation is optimal. The envelope is saturated. In multistep processes, terminal values may lie inside the extrema already visited by the path, and the history of branching constrains how terminal endpoints can be distributed across different envelope classes. These two effects produce the two nonnegative gap terms.

The martingale assumption used here places the results in the same setting as modern martingale formulations of stochastic thermodynamics. Entropy-production martingales have been used to derive universal results on infima, stopping times, and extreme-value statistics of entropy production [13–19]. The present work asks a comple-

mentary question. Rather than bounding the probability or expectation of the extrema themselves, it asks how those path extrema constrain the terminal mean entropy production. In this sense, the paper connects extrema statistics to upper bounds on dissipation.

The results are also complementary to thermodynamic uncertainty relations, speed limits, and inference bounds. Those approaches typically provide lower bounds on entropy production from currents, precision, dynamical activity, probability-flow geometry, or partial observations [2, 3, 5–7, 9, 10]. The present bounds address the upper-bound side: given information about path extrema, how large can the mean entropy production be? Both directions are useful. A lower bound certifies the minimum dissipation required by observed behavior; an upper bound constrains how much mean dissipation is compatible with the available entropy-production extremes.

Several limitations should be emphasized. First, the path-extrema results require the martingale property of $e^{-\Sigma_t}$, not merely the fixed-time fluctuation theorem. The deterministic endpoint support bound requires only $\langle e^{-\Sigma_T} \rangle = 1$, but the random path-extrema envelope uses the full process over $[0, T]$. Standard stationary Markov jump processes with local detailed balance provide a central physical class in which this condition holds, as do steady-state diffusion models under the usual stochastic-thermodynamic regularity assumptions. Second, the upper envelope \mathcal{U}_{ext} is a static relaxation over envelope classes. Its general dynamic attainability is a separate martingale-realizability problem, related in spirit to martingale transport and embedding questions. We have identified equality classes, such as one-step martingales, but do not claim universal dynamic sharpness. Third, the usefulness of any extrema-based bound depends on how well the relevant extrema or envelope statistics can be estimated or controlled in a physical experiment.

From an empirical point of view, the required observables are trajectory-level but not conceptually exotic. In a fully resolved Markov jump experiment, one accumulates Σ_t from the log ratio of forward and reverse transition rates and records the running extrema of $M_t = e^{-\Sigma_t}$. In a simulation, the same data are obtained directly from the generated jump record or diffusion path. The pair (L_T, H_T) can then be histogrammed or coarse-grained, the conditional mean $\mathbb{E}[M_T | L_T, H_T]$ estimated by binning, and the knapsack envelope computed by sorting bins according to ρ_T . Finite-sample uncertainty enters mainly through rare negative entropy-production excursions, which control large values of H_T and therefore can dominate the martingale-cost budget.

Long-time behavior is another open direction. In stationary nonequilibrium processes, $\langle \Sigma_T \rangle$ typically grows extensively in T with rate equal to the steady entropy-production rate. The quantities \mathcal{U}_{ext} , \mathcal{A} , and \mathcal{C} can also be studied at the level of asymptotic rates, but their scaling is not fixed by the mean entropy-production rate alone. The upper envelope is sensitive to rare entropy-consuming excursions through H_T , while the two gap

terms depend on terminal placement relative to the path-generated extrema and on the dynamic realizability of the optimal envelope allocation. Determining when these terms have well-defined linear growth rates, sublinear corrections, or extreme-value scaling is a natural problem for future work.

The last point suggests a natural future direction. Modern thermodynamic inference often works with partial data. The present results assume access to entropy-production path extrema, or at least to their statistical distribution. In practical settings, one may observe only coarse-grained currents, transition counts, waiting times, or finite-resolution trajectory snippets. It would be useful to combine lower-bound inference methods with statistically controlled estimates of path-extrema upper envelopes, thereby producing two-sided feasible intervals for mean entropy production. The gap decomposition may help in this task by identifying which part of the gap is due to terminal interiority and which part is due to cross-envelope allocation.

In summary, the main message is that the upper-bound side of entropy-production bounds is governed by path extrema and by how terminal entropy production sits within those extrema. The running extrema of $e^{-\Sigma_t}$ define an upper envelope, and the actual mean entropy production falls below it by two explicit nonnegative gap terms. This gives a structural counterpart to the usual lower-bound role of fluctuation relations and provides a pathwise interpretation of extrema-based upper bounds.

VIII. CONCLUSION

We have derived upper bounds on mean entropy production from the path extrema of the exponential entropy-production martingale. A one-sided bound on the positive entropy-production maximum gives no improvement over the trivial endpoint bound, because rare negative entropy-production trajectories can carry the exponential weight required by the fluctuation theorem. A deterministic two-sided entropy-production range gives a nontrivial secant-line upper bound, recovering the structure of earlier extrema-based results.

For random path extrema, the running minimum and maximum of $M_t = e^{-\Sigma_t}$ define an upper envelope \mathcal{U}_{ext} . This envelope is obtained from a continuous knapsack problem over realized extrema classes, with efficiency ratio $\ln(H_T/L_T)/(H_T - L_T)$. The actual mean entropy production satisfies the exact decomposition

$$\langle \Sigma_T \rangle = \mathcal{U}_{\text{ext}} - \mathcal{A} - \mathcal{C}.$$

Here $\mathcal{A} \geq 0$ is a cross-envelope allocation gap and $\mathcal{C} \geq 0$ is a within-envelope curvature gap. The decomposition separates the envelope set by path extrema from the two dynamical ways real processes fall below it: nonoptimal allocation across envelope classes and terminal placement inside realized intervals.

These results show that upper bounds on entropy production are not determined by terminal fluctuation relations alone. They depend on the extrema created along the path and on the terminal placement of the process within those extrema. The framework applies directly to stochastic-thermodynamic models in which $e^{-\Sigma_t}$ is a positive entropy-production martingale, including stationary Markov jump processes with local detailed balance. This provides a path-extrema framework for upper bounds in stochastic thermodynamics and identifies concrete observables that can be estimated from resolved trajectory data.

The resulting picture is simple: path extrema set the thermodynamic room available to the endpoint, martingale normalization determines how that room can be spent across trajectories, and the actual dynamics determine how much of the relaxed envelope is lost through allocation and curvature gaps.

Appendix A: Notation summary

For reference, we collect the main quantities used in the paper:

$$M_t = e^{-\Sigma_t}, \quad L_T = \inf_{0 \leq t \leq T} M_t, \quad H_T = \sup_{0 \leq t \leq T} M_t.$$

The entropy-production extrema, conditional terminal mean, and actual envelope-conditioned endpoint weight are

$$\begin{aligned} A_T &= -\ln L_T, & B_T &= \ln H_T, \\ \mu_T &= \mathbb{E}[M_T | L_T, H_T], \\ r_T &= \frac{H_T - \mu_T}{H_T - L_T}. \end{aligned}$$

The path-extrema upper envelope is

$$\begin{aligned} \mathcal{U}_{\text{ext}} &= \langle -\ln H_T \rangle \\ &+ \sup_{0 \leq r \leq 1} \left\{ \left\langle r \ln \frac{H_T}{L_T} \right\rangle : \langle r(H_T - L_T) \rangle = \langle H_T \rangle - 1 \right\}. \end{aligned}$$

The efficiency ratio is

$$\rho_T = \frac{\ln(H_T/L_T)}{H_T - L_T} = \frac{A_T + B_T}{e^{B_T} - e^{-A_T}}.$$

The allocation and curvature gaps are

$$\mathcal{A} = \left\langle (r_T^* - r_T) \ln \frac{H_T}{L_T} \right\rangle,$$

and

$$\mathcal{C} = \langle \ell_{L_T, H_T}(M_T) - (-\ln M_T) \rangle.$$

The central decomposition is

$$\langle \Sigma_T \rangle = \mathcal{U}_{\text{ext}} - \mathcal{A} - \mathcal{C}.$$

Appendix B: Continuous-knapsack optimizer

This appendix gives the standard derivation of the optimizer used in Eq. (7). Let

$$c_T = \ln \frac{H_T}{L_T}, \quad d_T = H_T - L_T, \quad K = \langle H_T \rangle - 1.$$

The optimization problem is

$$\sup_{0 \leq r \leq 1} \langle r c_T \rangle$$

subject to

$$\langle r d_T \rangle = K.$$

Assume first that $d_T > 0$ almost surely on the nontrivial part of the sample space. Define

$$\rho_T = \frac{c_T}{d_T}.$$

Then

$$\langle r c_T \rangle = \langle r \rho_T d_T \rangle.$$

Introduce the measure

$$d\nu = d_T d\mathbb{P}.$$

The constraint and objective become

$$\int r d\nu = K, \quad \int r \rho_T d\nu.$$

Thus the optimizer chooses $r = 1$ on the largest values of ρ_T , then on progressively smaller values, with possible partial assignment at the threshold. Equivalently, if $\rho^*(u)$ denotes the decreasing rearrangement of ρ_T with respect to ν , then

$$\sup_{0 \leq r \leq 1, \int r d\nu = K} \int r \rho_T d\nu = \int_0^K \rho^*(u) du.$$

This gives the rearrangement form

$$\mathcal{U}_{\text{ext}} = \langle -\ln H_T \rangle + \int_0^{\langle H_T \rangle - 1} \rho^*(u) du.$$

The threshold form follows equivalently from a Lagrange multiplier. Consider

$$\langle r c_T \rangle - \lambda \langle r d_T \rangle = \langle r(c_T - \lambda d_T) \rangle.$$

Pointwise maximization over $0 \leq r \leq 1$ gives

$$r_T^* = \begin{cases} 1, & c_T - \lambda d_T > 0, \\ 0, & c_T - \lambda d_T < 0, \\ \theta_T \in [0, 1], & c_T - \lambda d_T = 0. \end{cases}$$

Since $c_T - \lambda d_T = d_T(\rho_T - \lambda)$, this is the threshold rule stated in the main text.

Appendix C: Algebra of the gap decomposition

Here we spell out the algebra behind Eq. (16). Let

$$\mu_T = \mathbb{E}[M_T \mid L_T, H_T]$$

and

$$r_T = \frac{H_T - \mu_T}{H_T - L_T}.$$

The secant line of $f(m) = -\ln m$ over $[L_T, H_T]$ is

$$\ell_{L_T, H_T}(m) = \frac{H_T - m}{H_T - L_T} f(L_T) + \frac{m - L_T}{H_T - L_T} f(H_T).$$

Conditioning on (L_T, H_T) gives

$$\begin{aligned} \mathbb{E}[\ell_{L_T, H_T}(M_T) \mid L_T, H_T] \\ = \frac{H_T - \mu_T}{H_T - L_T} f(L_T) + \frac{\mu_T - L_T}{H_T - L_T} f(H_T). \end{aligned}$$

Using the definition of r_T ,

$$\begin{aligned} \mathbb{E}[\ell_{L_T, H_T}(M_T) \mid L_T, H_T] &= r_T(-\ln L_T) \\ &\quad + (1 - r_T)(-\ln H_T) \\ &= -\ln H_T + r_T \ln \frac{H_T}{L_T}. \end{aligned}$$

Averaging gives

$$\langle \ell_{L_T, H_T}(M_T) \rangle = \mathcal{U}_{\text{cond}}.$$

By definition,

$$\mathcal{C} = \langle \ell_{L_T, H_T}(M_T) - (-\ln M_T) \rangle,$$

so $\langle \Sigma_T \rangle = \mathcal{U}_{\text{cond}} - \mathcal{C}$.

Similarly,

$$\mathcal{U}_{\text{ext}} = \langle -\ln H_T \rangle + \left\langle r_T^* \ln \frac{H_T}{L_T} \right\rangle,$$

while

$$\mathcal{U}_{\text{cond}} = \langle -\ln H_T \rangle + \left\langle r_T \ln \frac{H_T}{L_T} \right\rangle.$$

Thus

$$\mathcal{U}_{\text{ext}} - \mathcal{U}_{\text{cond}} = \left\langle (r_T^* - r_T) \ln \frac{H_T}{L_T} \right\rangle = \mathcal{A}.$$

Combining these identities yields

$$\langle \Sigma_T \rangle = \mathcal{U}_{\text{ext}} - \mathcal{A} - \mathcal{C}.$$

Appendix D: Details for the two-stage tree

For the two-stage martingale tree in Sec. VIC, the four terminal outcomes are

$$(M_T, L_T, H_T, p) = \left(\frac{1}{4}, \frac{1}{4}, 1, \frac{1}{3} \right), \left(\frac{3}{4}, \frac{1}{2}, 1, \frac{1}{3} \right), \\ \left(\frac{3}{2}, 1, 2, \frac{2}{9} \right), \left(3, 1, 3, \frac{1}{9} \right).$$

The actual mean entropy production is

$$\langle \Sigma_T \rangle = \frac{1}{3} \ln 4 + \frac{1}{3} \ln \frac{4}{3} - \frac{2}{9} \ln \frac{3}{2} - \frac{1}{9} \ln 3 \simeq 0.345821.$$

The martingale-cost budget is $K = \langle H_T \rangle - 1$. Here

$$\langle H_T \rangle = \frac{1}{3}(1) + \frac{1}{3}(1) + \frac{2}{9}(2) + \frac{1}{9}(3) = \frac{13}{9},$$

so $K = 4/9$. The envelope classes, costs, and efficiency ratios are

(L, H)	p	$p(H - L)$	$\rho = \ln(H/L)/(H - L)$
(1/4, 1)	1/3	1/4	$\ln 4/(3/4)$
(1/2, 1)	1/3	1/6	$\ln 2/(1/2)$
(1, 2)	2/9	2/9	$\ln 2$
(1, 3)	1/9	2/9	$\ln 3/2$

The costs of the first two classes add to $1/4 + 1/6 = 5/12$. The remaining budget is $4/9 - 5/12 = 1/36$. Thus the optimal allocation uses the first two classes fully and uses a fraction $(1/36)/(2/9) = 1/8$ of the third class. Hence $r^* = (1, 1, 1/8, 0)$ on the four classes in decreasing order of ρ .

The path-extrema upper envelope is therefore

$$\mathcal{U}_{\text{ext}} = \langle -\ln H_T \rangle + \left\langle r^* \ln \frac{H_T}{L_T} \right\rangle.$$

The first term is $\langle -\ln H_T \rangle = -\frac{2}{9} \ln 2 - \frac{1}{9} \ln 3$, and the second term is $\frac{1}{3} \ln 4 + \frac{1}{3} \ln 2 + \frac{2}{9} \cdot \frac{1}{8} \ln 2$. Therefore

$$\mathcal{U}_{\text{ext}} = \frac{1}{3} \ln 4 + \left(\frac{1}{3} + \frac{1}{36} - \frac{2}{9} \right) \ln 2 - \frac{1}{9} \ln 3.$$

Numerically,

$$\mathcal{U}_{\text{ext}} \simeq 0.436301.$$

We next compute the actual conditional allocation weights r_T . In this discrete example, each envelope class contains one terminal outcome, so

$$r_T = \frac{H_T - M_T}{H_T - L_T}.$$

Thus $r_T = (1, 1/2, 1/2, 0)$ on the four classes. The allocation gap is

$$\mathcal{A} = \left\langle (r^* - r_T) \ln \frac{H_T}{L_T} \right\rangle.$$

Only the second and third classes contribute:

$$\mathcal{A} = \frac{1}{3} \left(1 - \frac{1}{2} \right) \ln 2 + \frac{2}{9} \left(\frac{1}{8} - \frac{1}{2} \right) \ln 2.$$

Thus $\mathcal{A} = (1/6 - 1/12) \ln 2 = (1/12) \ln 2 \simeq 0.057762$.

The curvature gap is

$$\mathcal{C} = \langle \ell_{L_T, H_T}(M_T) - (-\ln M_T) \rangle.$$

Only the two interior terminal outcomes contribute. For

$$(L, H, M) = (1/2, 1, 3/4),$$

$$\ell_{1/2, 1}(3/4) = \frac{1}{2} \ln 2,$$

while

$$-\ln(3/4) = \ln \frac{4}{3}.$$

The contribution is $\frac{1}{3} \left[\frac{1}{2} \ln 2 - \ln \frac{4}{3} \right]$. For $(L, H, M) = (1, 2, 3/2)$,

$$\ell_{1, 2}(3/2) = -\frac{1}{2} \ln 2,$$

while

$$-\ln(3/2) = -\ln \frac{3}{2}.$$

The contribution is $\frac{2}{9} \left[-\frac{1}{2} \ln 2 + \ln \frac{3}{2} \right]$. Hence

$$\mathcal{C} = \frac{1}{3} \left[\frac{1}{2} \ln 2 - \ln \frac{4}{3} \right] + \frac{2}{9} \left[-\frac{1}{2} \ln 2 + \ln \frac{3}{2} \right] \simeq 0.032718.$$

Therefore

$$\mathcal{A} + \mathcal{C} \simeq 0.090480 = \mathcal{U}_{\text{ext}} - \langle \Sigma_T \rangle,$$

as stated in the main text.

Appendix E: Envelope distribution

Figure 4 shows the empirical distribution of realized envelope classes used in the appendix-level diagnostics for the Markov-jump example. The axes are the entropy extrema $A_T = -\ln L_T$ and $B_T = \ln H_T$; color gives the efficiency ratio ρ , marker area indicates empirical weight, open circles show selected bins, and the red diamond marks the threshold bin. This figure is diagnostic rather than part of the proof; it displays the sampled envelope population underlying the empirical knapsack construction.

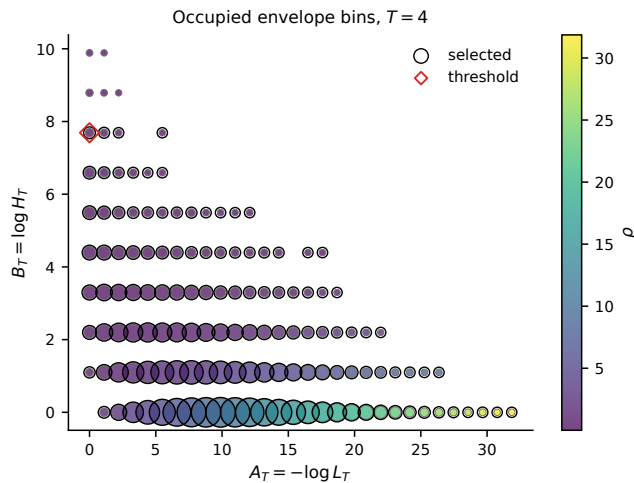


FIG. 4. Appendix-level diagnostic showing the empirical distribution of realized envelope classes in the Markov-jump example. Each occupied bin is plotted in entropy-extrema coordinates (A_T, B_T) , with color indicating the efficiency ratio ρ and marker area indicating empirical weight. Open circles mark bins selected by the knapsack sorting, and the red diamond marks the threshold bin. This diagnostic supports the interpretation of Fig. 2 and shows that the upper-envelope estimate is built from occupied envelope bins rather than a formal continuum.

-
- [1] U. Seifert, *Physical Review Letters* **95**, 040602 (2005).
[2] A. C. Barato and U. Seifert, *Physical Review Letters* **114**, 158101 (2015).
[3] T. R. Gingrich, J. M. Horowitz, N. Perunov, and J. L. England, *Physical Review Letters* **116**, 120601 (2016).
[4] J. M. Horowitz and T. R. Gingrich, *Nature Physics* **16**, 15 (2020).
[5] N. Shiraishi, K. Funo, and K. Saito, *Physical Review Letters* **121**, 070601 (2018).
[6] A. Dechant and S.-i. Sasa, *Journal of Statistical Mechanics: Theory and Experiment* **2018**, 063209 (2018).
[7] G. Bisker, M. Poletti, T. R. Gingrich, and J. M. Horowitz, *Journal of Statistical Mechanics: Theory and Experiment* **2017**, 093210 (2017).
[8] U. Seifert, *Annual Review of Condensed Matter Physics* **10**, 171 (2019).
[9] P. E. Harunari, S. Dutta, M. Poletti, and E. Roldán, *Physical Review X* **12**, 041026 (2022).
[10] S. Singh, D. J. Skinner, and J. M. Horowitz, *Communications Physics* **7**, 261 (2024).
[11] S. Limkumnerd, *Physical Review E* **95**, 032125 (2017).
[12] T. Nishiyama and Y. Hasegawa, *Physical Review E* **108**, 044139 (2023).
[13] E. Roldán, I. Neri, M. Dörpinghaus, H. Meyr, and F. Jülicher, *Physical Review Letters* **115**, 250602 (2015).
[14] I. Neri, E. Roldán, and F. Jülicher, *Physical Review X* **7**, 011019 (2017).
[15] S. Pigolotti, I. Neri, E. Roldán, and F. Jülicher, *Physical Review Letters* **119**, 140604 (2017).
[16] I. Neri, E. Roldán, S. Pigolotti, and F. Jülicher, *Journal of Statistical Mechanics: Theory and Experiment* **2019**, 104006 (2019).
[17] I. Neri, *Physical Review Letters* **124**, 040601 (2020).
[18] G. Manzano and E. Roldán, *Physical Review E* **105**, 024112 (2022).
[19] E. Roldán, I. Neri, R. Chetrite, S. Gupta, S. Pigolotti, F. Jülicher, and K. Sekimoto, *Advances in Physics* **72**, 231 (2024).
[20] U. Seifert, *Reports on Progress in Physics* **75**, 126001 (2012).
[21] M. Beiglböck and N. Juillet, *Annals of Probability* **44**, 42 (2016).